A R C H I V E S O F M E T A L L U R G Y A N D M A T E R I A L S
Volume 54 2009 Issue 1

E. FRAŚ*, M. GÓRNY*, H. F. LOPEZ**

MECHANISM OF THE SILICON INFLUENCE ON ABSOLUTE CHILLING TENDENCY AND CHILL OF CAST IRON

MECHANIZM WPŁYWU KRZEMU NA BEZWZGLĘDNĄ SKŁONNOŚĆ ŻELIWA DO ZABIELEŃ I ZABIELENIA W ŻELIWIE

In this work an analytical solution of general validity is used to explain mechanism of the silicon influence on the absolute chilling tendency (CT) and chill (w) of cast iron. It is found that CT can be related to nucleation potential of graphite (N_v), growth parameter (μ) of eutectic cells, temperature range (ΔT_{sc}), where $\Delta T_{sc} = T_s - T_c$ (T_s is graphite eutectic equilibrium temperature and T_c is cementite eutectic formation temperature) and the pre-eutectic austenite volume fraction (f_γ). It has been shown that silicon addition: 1) impedes the growth of graphite eutectic cells through decreasing the graphite eutectic growth coefficient (μ), 2) expands the temperature range (ΔT_{sc}), 3) increases the nucleation potential of graphite (N_v), 4) lowers the pre-eutectic austenite volume fraction, (f_γ). In a consequence, the absolute chilling tendency (CT) decreases. The minimum wall thicknesses for chilled castings, or chill width (w) in wedge shaped castings is related to CT and as Si content increases, the chill width, w value decreases.

Keywords: cast iron, chilling tendency, chill

W pracy przedstawiono wyniki rozwiązania analitycznego mechanizmu wpływu krzemu na bezwzględną skłonność żeliwa do zabieleń (CT) i zabielenia (w) w żeliwie. Wykazano, że CT jest uzależnione od potencjału zarodkowania grafitu (N_v), parametru wzrostu (μ) ziaren eutektycznych, zakresu temperatury (ΔT_{sc}), gdzie $\Delta T_{sc} = T_s - T_c$ (T_s jest równowagową temperaturą krystalizacji eutektyki grafitowej, a T_c jest temperaturą tworzenia eutektyki cementowej) oraz udział przedeutektycznego austenitu (f_γ). Z przedstawionych badań wynika, że dodatek krzemu: 1) utrudnia wzrost ziaren eutektycznych poprzez zmniejszenie współczynnika wzrostu eutektyki grafitowej (μ), 2) rozszerza zakres temperatury (ΔT_{sc}), 3) zwiększa potencjał zarodkowania grafitu (N_v, 4) zmniejsza udział przedeutektycznego austenitu (f_γ) a w konsekwencji zmniejsza bezwzględną skłonność żeliwa do zabieleń (CT). Wykazano ponadto, że minimalna grubość ścianki, powyżej której w odlewie występują zabielenia lub szerokość zabielenia klina (w) w odlewie o kształcie klina zależy od CT oraz zwiększenie zawartości krzemu prowadzi do zmniejszenia szerokości zabielania klina.

1. Introduction

One of the important indices of quality of cast iron is its chilling tendency, that is its tendency to solidify according to Fe-C-X metastable system. Chilling tendency depends on physical-chemical state of liquid cast iron while chill (fraction of cementite eutectic in casting) formation depends additionally on cooling rate of casting.

In the foundry practice, the chilling tendency for the various types of cast irons is determined from comparisons of the exhibited fraction of cementite eutectic (chill) in castings solidified under similar cooling rate. Figure 1 gives a comparison of the chilling tendency for two cast irons (I and II). Cast iron I exhibits a lower chilling tendency than cast iron II. Based only on this comparison, the difference in the chilling tendency of

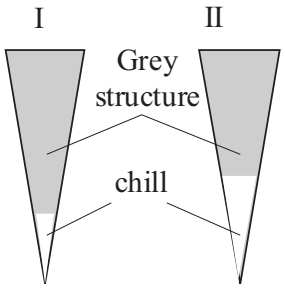

Fig. 1. Castings according to ASTM standard for chill and chilling tendency estimation

* AGH UNIVERSITY OF SCIENCE AND TECHNOLOGY, 30-059 KRAKÓW, 23 REYMONTA STR., POLAND
** UNIVERSITY OF WISCONSIN-MILWAUKEE, P.O. BOX 784, MILWAUKEE, WI 53201, USA

various cast irons can be established, but absolute chilling tendency (CT) values for given irons cannot be derived.

It is well known that the chilling tendency of cast iron determines their subsequent performance in various applications. In particular, cast irons possessing a high chilling tendency tend to develop zones of white or mottled iron. Considering that these regions can be extremely hard, their machinability can be severely impaired. Alternatively, if white iron is the desired structure a relatively small chilling tendency will favour the formation of gray iron. This in turn leads to low hardness and poor wear properties in as-cast components. Hence, considerable efforts (Fuller, 1961, Boyes, 1964, Girshovitz, 1966, Merchant, 1968, Davson, 1976, Fras, 1990, Kubick, 1997) have been made in correlating the inoculation practice, iron composition, pouring temperature, etc. with the chilling tendency of cast iron. On the other hand only a few attempts aimed at elucidating the mechanisms responsible for the chill of cast iron (Oldfield, 1962, Girshovitz, 1966, Hillert, 1968, Magnin, 1985, Fredriksson, 1985). Nevertheless, none of these hypotheses have taken into consideration the complexity of the solidification process. In most cases, the proposed theories assume that a single factor is determinant in establishing the solidification structure while the remaining factors are ignored. In addition, various numerical models have been proposed (Nastac, 1995, Nastac, 1997) to predict whether a given casting or part of it will solidify according to the stable or metastable Fe-C-X system. However, their application is tedious due to extensive numerical calculations. Accordingly, in this work a simple and common analytical model is used for the explanation of the mechanism responsible for the chilling tendency of cast iron and in consequence the chill.

2. Experimental procedure

The experimental melts were made in the electric induction furnace. The charge materials for the furnace consisted of pig iron, steel scrap, commercially pure silicon, and ferro-phosphorus. After melting of the charge and preheating to 1400 °C (2552 °F), the wedges (ASTM A367-55T standard) of the type (dimensions: B_w = 2.5 cm and β = 25 °) were cast. From each melt, a sample was taken for chemical composition (Table 1). A Pt-PtRh10 thermocouples was inserted in the center of the wedge cavity in the sand mold and an Agilent 34970A electronic module was employed for numerical temperature recording. Figure 2 shows typical cooling curve and their first derivative, where characteristic points are shown i.e. initial metal temperature T_i just after filling of mold, minimal temperature T_m at the onset of graphite eutectic solildification and cooling rate Q at the graphite eutectic equilibrium temperature T_s. Cooling curves were used for determinations of the initial metal temperature, T_i just after filling of mold (Table 1).

TABLE 1

Silicon content and results of measurements

No.	Si %	T_i °C	$N_{F,cr}$ cm^{-2}	$N_{V,cr}$ cm^{-3}	w mm
1	1.50	1260	182	1394	12.5
2	1.95	1230	299	2937	9.6
3	2.12	1225	821	13362	7.4
4	2.48	1220	871	14600	6.7
5	3.18	1270	1112	21062	4.3
Average chemical composition (wt. %) C= 3.23%, P= 0.08% Mn = 0.11; S = 0.04%					

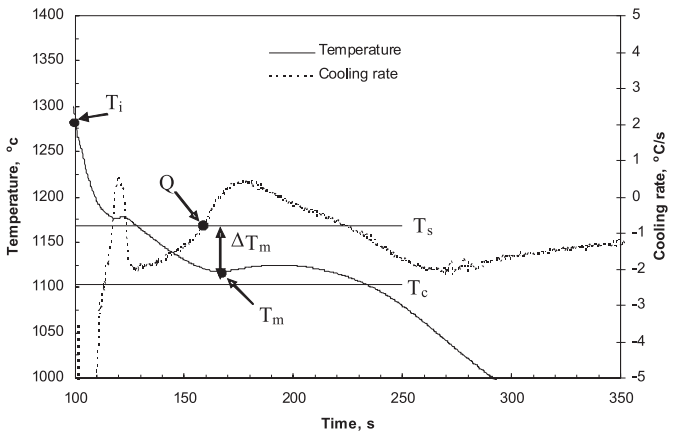

Fig. 2. Cooling curve and their first derivative for cast iron

After cooling, specimens for metallographic examination were taken from the wedges. Metallographic examinations were made on polished cross-sections of wedges (Fig 3). After etching using nital, width of wedge (w) was determined for which the last precipitates of cementite are still present (total chill) (Fig 3). Next samples were polished again and etched using Stead reagent to reveal graphite eutectic cell boundaries (Fig 3). The planar microstructure was characterized by the cell count, N_F which gives the average number of graphite eutectic cells per unit area. The N_F parameter can be determined by means of so-called variant II of the Jeffries method, and applying the Saltykov formula as an unbiased estimator for the rectangle S of observation (Ryś, 1995) .

$$N_F = \frac{N_i + 0.5\, N_r + 1}{F} \tag{1}$$

where: N_i is the number of eutectic cells inside rectangle S (Fig. 3a), N_r is the number of eutectic cells that intersect the sides of the rectangle S but not their corners and F is the surface area of the rectangle S.

The graphite eutectic cells have a granular microstructure, and it can be assumed that the spatial grain configurations follow the so-called Poisson-Voronoi model(Ryś, 1996). Then, a stereological formula can be employed for calculations of the volumetric cell count N_V, which yields the average number of eutectic cells per unit volume.

$$N_V = 0.568(N_F)^{3/2} \tag{2}$$

The chilled iron at the apex of the wedge consisted of two zones; (1) the portion closest to the apex was entirely free of any gray spots and it was designated as a clear chill, and (2) the portion starting at the end of the clear chill and continuing all the way down to the location where the last spot of cementite that is white iron is visible was designated as the mottled zone. The width, w of the total chill and the cell count, $N_{F,cr}$ were measured at the junction of the gray cast iron microstructure with the first appearance of chilled iron, see Fig. 3 (near the cementite eutectic formation temperature, T_c). The planar cell count, $N_{F,cr}$ in the vicinity of that junction was converted into the volumetric cell count, $N_{V,cr}$ using Eq. 2. The results of these measurements are given in Table 1.

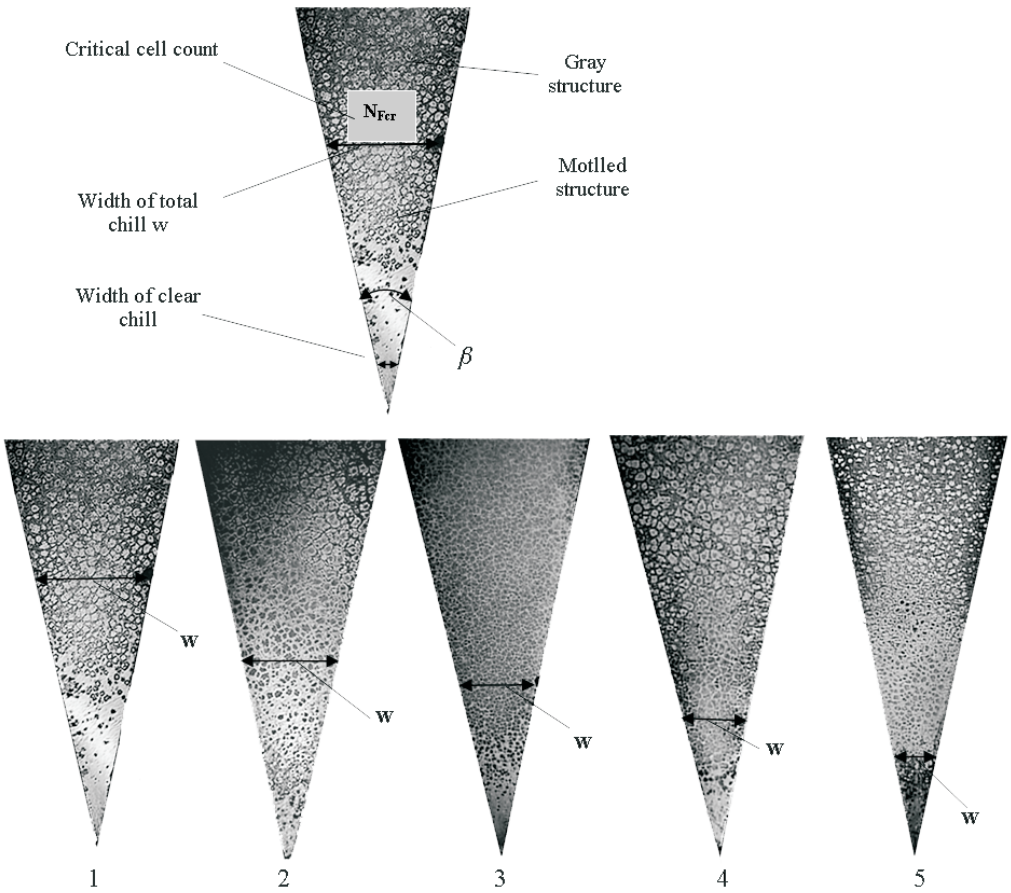

Fig. 3. Microstructures in wedge shaped castings from test melts 1-5

3. Analysis

The minimal temperature, T_m at the onset of graphite eutectic solidification (see Fig. 2) can be calculated from equation proposed by Fraś et al. (Fraś, 2007):

$$T_m = T_s - \Delta T_m = T_s - \left(\frac{4\, c_{ef}\, Q}{\pi^3\, L_e\, N_v\, \mu^3 (1 - f_\gamma)} \right)^{1/8} \tag{3}$$

where

$$Q = \frac{2\, T_s\, a^2}{\pi \phi\, c_{ef}\, M^2} \tag{4}$$

$$\Delta T_m = T_s - T_m \tag{5}$$

$$c_{ef} = c + \frac{L_\gamma}{T_{l\gamma} - T_s} \tag{6}$$

$$\phi = c\, B + c_{ef}\, B_1 \tag{7}$$

$$B = \ln \frac{T_i}{T_l};\quad B_1 = \ln \frac{T_l}{T_S} \tag{8}$$

$$M = \frac{V_C}{F_C} \tag{9}$$

In above equations, ΔT_m is the maximum degree of undercooling at the onset of graphite eutectic solildification (Fig. 2), Q is the cooling rate of cast iron at temperature, T_s (Fig. 2), M is the casting modulus, V_c and F_c are volume and surface area of the casting, respectively, f_γ is the volumetric fraction of pre-eutectic austenite, T_i is the initial liquid metal temperature just after pouring into the mold (Fig. 2), T_m is the minimal temperature at the onset of graphite eutectic solildification (Fig. 2) and T_s, T_l, $T_{l\gamma}$, a, c, L_e, L_γ,, μ_g are defined in Table 2.

TABLE 2

Selected thermophysical data used in calculations

Parameter	Value and units
Latent heat of graphite eutectic	L_e = 2028.8; J/cm^3
Latent heat of austenite	L_γ = 1904.4; J/cm^3
Specific heat of cast iron	c = 5.95; J/(cm^3 °C)
Growth coefficient of graphite eutectic	$\mu = 10^{-6}$ (0.2 - 6.3 Si) $^{0.25}$; cm/(°C^2 s)
Material mould ability to absorb heat	a = 0.10; J/(cm^2 s$^{1/2}$ °C)
Liquidus temperature for pre-eutectic austenite	T_l = 1636 - 113(C + 0.25Si + 0.5P); °C
Graphite eutectic equilibrium temperature	T_s = 1154.0 + 5.25Si - 14.88P; °C
Cementite eutectic formation temperature	T_c = 1130.56 + 4.06(C - 3.33Si - 12.58 P); °C
$\Delta T_{sc} = T_s - T_c$	ΔT_{sc} = 23.34 - 4.07C +18.80Si + 36.29P; °C
Carbon content in graphite eutectic	C_e = 4.26 - 0.30Si - 0.36P; wt, %
Maximum carbon content in austenite at T_s	C_γ = 2.08 - 0.11Si - 0.35P, wt, %
Liquidus temperature of pre-eutectic austenite when its composition is C_γ	$T_{l\gamma}$ = 1636 -113(2.08 + 0.15Si + 0.14P); °C
Austenite density	ρ_γ = 7.51 g/cm^3
Melt density	ρ_m = 7.1 g/cm^3
C,Si,P – content of carbon, silicon and phosphorus in cast iron, respectively, wt, %	

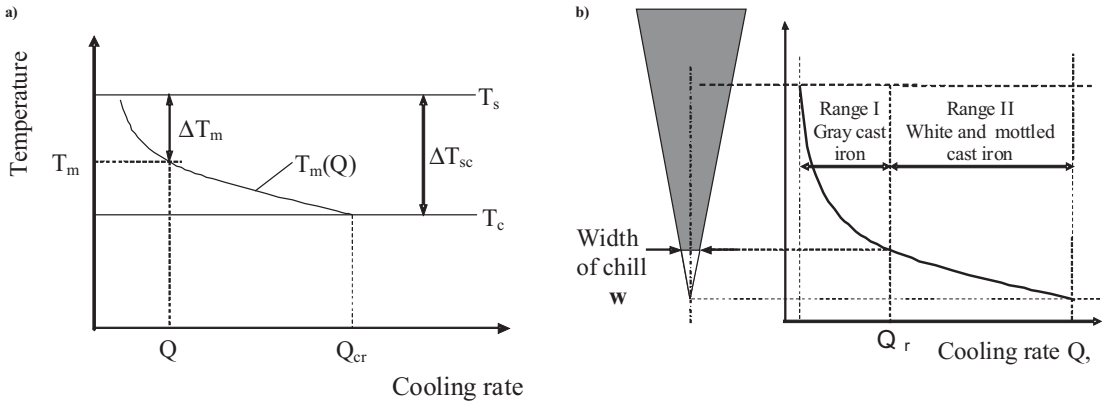

Fig. 4. Effect of the cooling rate Q on the minimal solidification temperature, T_m for graphite eutectic (a) and scheme of the wedge section and cooling rate along its axis (b)

Figure 4a is schematic representation of the cooling rate Q on temperature T_m. Note, from this figure, that increasing the cooling rates, Q to values equal to Q_{cr}, leads to a reduction in, T_m to values equal to T_c (cementite eutectic formation temperature, Table 2) and hence to the formation of cementite eutectic (chill development). It can be concluded that the wider the temperature range, ΔT_{sc}, the higher the critical cooling rate, Q_{cr} needed for the development of chill in the casting. Under these conditions, it is expected that the chill widths to be produced in wedge shaped castings will be relatively small.

Absolute chilling tendency CT of cast iron

From Fig. 4 results that for $Q = Q_{cr}$, $\Delta T_m = \Delta T_{sc}$ and the absolute chilling tendency of cast iron is given (Fraś, 2007) by the fllowing equation:

$$CT = \left[\frac{1}{N_{V,cr}\left(1-f_\gamma\right)\mu_g^3\Delta T_{sc}^8}\right]^{1/6} = f(Si) \qquad (10)$$

where $N_{V,cr}$ is the critical cell count at $T \approx T_c$ (close to chill, see Fig. 3, and Table 1)

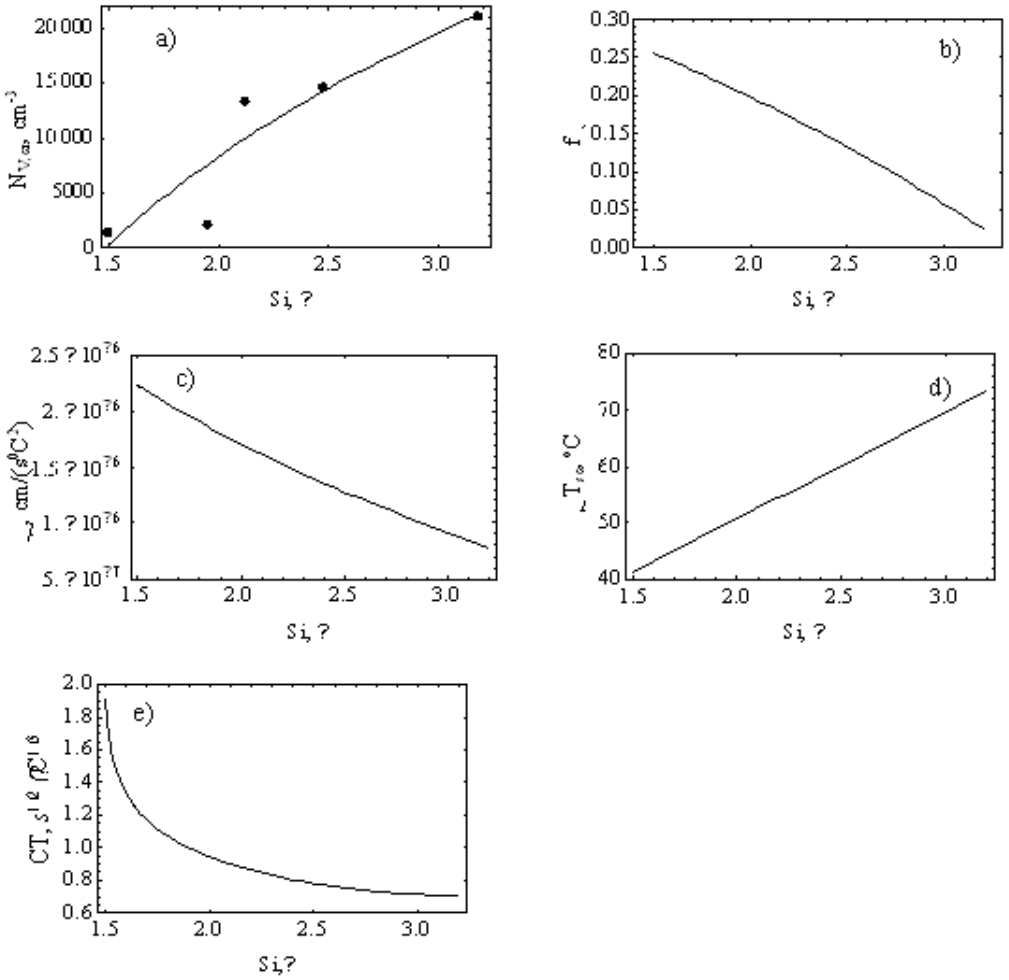

Fig. 5. Effect of silicon on the critical cell count, $N_{V,cr}$, (a), the volumetric fraction of pre-eutectic austenite, f_γ, (b) the growth coefficient of graphite eutectic, μ, (c), temperature range, ΔT_{sc}, (d) and the absolute chilling tendency, CT, (e)

From the theoretical perspective, the role of the silicon on the chilling tendency CT of cast iron can be disclosed based on Eq. (10)

- ***The critical cell count***, $\mathbf{N_{V,cr}}$. It is well known that each nucleus graphite gives rise to a single eutectic cell, so it can be assumed that measure of graphite nuclei count is eutectic cell count. An increase in the cell count means that, for a given cooling rate, during eutectic transformation the nucleation potential of graphite also increases. Figure 5a shows the relation between silicon content in cast iron and the critical cell count, $N_{V,cr}$. In particular, on the basis

of experimental research it can be concluded that as silicon contents increase the, $N_{V,cr}$ also increase and according to Eq. (10) decrease absolute chilling tendency of cast iron.

- ***The effect of the volumetric fraction of pre-eutectic austenite*** $\mathbf{f}_\gamma$. The volumetric fraction of pre-eutectic austenite can be obtained from carbon mass balance and described by

$$f_\gamma = \frac{\rho_\gamma \, g_\gamma}{\rho_\gamma + g_\gamma \, (\rho_m - \rho_\gamma)}, \tag{11}$$

where:

$$g_\gamma = \frac{C_e - C}{C_e - C_\gamma}, \tag{12}$$

g_γ is mass fraction of austenite, ρ_γ and ρ_m are the density of austenite and the melt (Table 2), and C_e and C_γ (Table 2) are the carbon content in the graphite eutectic and in the austenite at the graphite eutectic equilibrium temperature T_s

From calculations results that increasing the amount of silicon lowers the volume fraction of austenite (Fig. 5b), so from Eq. (10) it can be concluded that as f_γ decreases the absolute chilling tendency also decreases.

- ***The graphite eutectic growth coefficient*** μ, depends on the cast iron chemistry. However, with the exception of silicon, little is known about the influence of other elements on μ. Reported values for growth coefficient of graphite eutectic μ_g are given for Fe-C, Fe-C-0.1 % Si[1]) (Magnin, 1985), and Fe-C-2 % Si(Lux, 1967) systems. In general, silicon lowers the graphite eutectic growth coefficient (Table 2 and Fig. 5c) so as Si contents increases, μ decreases and from Eq. 10 results that the absolute chilling tendency of cast iron increases.
- ***The temperature range*** $\Delta T_{sc} = T_s - T_c$, (Table 2) depends on the melt chemistry. For a low value of phosphosus content in cast iron temperature range ΔT_{sc} can be described by

$$\Delta T_{sc} = 23.34 - 4.07C + 18.80Si°C. \tag{13}$$

From the above expression and Fig. 5d, it can be observed that as Si contents increases, the ΔT_{sc} range also increases, and from Eqs. 10 the absolute chilling tendency, CT of cast iron decreases.

Taking into account the chemical composition of the cast iron, the cell count, $N_{V,cr}$ (Table 1), equation (11) and data in Table 2 the absolute chilling tendency, CT can be estimated from Eq. 10. Results of these calculations are summarized in Table 3 and are shown in Fig. 5e. From this figure results that silicon most intensely changes the absolute chilling tendency, CT when occurring in the range up to 2 %. After crossing 3 % its influence on, CT is small.

TABLE 3

Measured and calculated results

No.	Si wt. %	μ cm/(s °C)	ΔT_{sc} °C	f_γ	CT $s^{1/2}/°C^{1/3}$	w, mm	
						measured	calculated
1	1.50	$2.2\ 10^{-6}$	41.3	0.27	1.48	12.5	10.8
2	1.95	$1.75\ 10^{-6}$	49.7	0.22	1.13	9.6	8.2
3	2.12	$1.59\ 10^{-6}$	52.9	0.19	0.84	7.4	6.4
4	2.48	$1.29\ 10^{-6}$	59.7	0.14	0.78	6.7	6.5
5	3.18	$7.9\ 10^{-7}$	72.9	0.02	0.70	4.3	5.6
C = 3.23 %, P = 0.08 %							

Chill

In the foundry practice an assessment of the chilling tendency of cast iron is based on the chill test methods established by the ASTM A367-55T standard. The total chill width of wedge is estimated(Fraś, 2005), by

$$w = A\ CT, \tag{14}$$

where

$$A = \frac{4n2^{5/6} a T_s^{1/2}}{\pi \phi^{1/2} c_{ef}^{1/3} L_e^{1/6} \cos(\beta/2)}, \tag{15}$$

where n is a wedge size coefficient and β is the wedge angle (Fig. 3), n = 0.68 , β =25 °

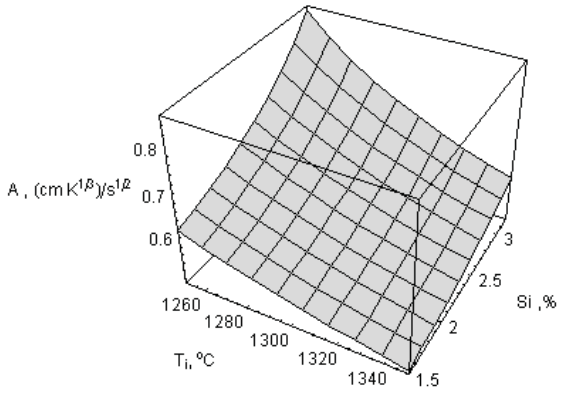

Fig. 6. Effect of silicon content and initial liquid metal temperature just after pouring into the mold, T_i on A parameter

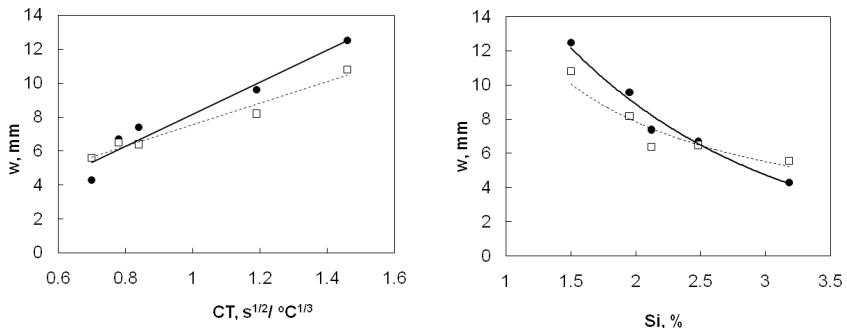

Fig. 7. Effect of absolute chilling tendency CT and silicon content on the total chill of wedges solid line- experimental values of w, dotted line – calculated values of w

Apart the absolute chilling tendency of cast iron CT, the wedge chill width w according to Eq. 14 depends additionally on the A coefficient (Eq. 15). It includes parameters connected with cooling rate (Eq. 4) that is:

- the ability of the mold to absorb heat, a,
- ϕ parameter which depends on B and B_1 values (Eq. 8) that is on the initial temperature, T_i of the cast iron just after pouring into the mold and on the liquidus temperature for pre-eutectic austenite, T_l and in consequence on silicon content (Table 2),
- Effective specific heat c_{ef} which also depends on silicon content (through liquidus temperature of pre-eutectic austenite, $T_{l\gamma}$ and graphite eutectic equilibrium temperature T_s (Table 2).

Influence of silicon and the initial temperature, T_i on values of A parameter is shown in Fig. 6. Thus, it can be concluded that chill, w increases as the ability of the mold to absorb heat, a increases. For a = const. increasing the pouring temperature T_p (and in consequence initial temperature T_i) lowers of, A parameter (Fig. 6). Effect of silicon on the absolute chilling tendency, CT is given by Eq. 10 and is shown in Fig. 5e. Using eqs. 10 and 14 the relationship between absolute chilling tendency or silicon content and width of chill is obtained (Fig. 7). One can say that the increase in silicon content in cast iron decreases absolute chilling tendency, CT and in consequence the width of chill, w. Moreover, from investigations results that intensity of silicon influence on absolute chilling tendency, CT and width of chill, w lowers as silicon content in cast iron increases. It is worth to mention that the theoretical predictions of this work are in agreement with the experimental data (Fig. 7).

4. Conclusions

In this work the theory which explains mechanism of influence of different technological parameters on absolute chilling tendency (CT) and chill in cast iron is presented. Theory was experimentally verified using silicon as an example. In particular, it has been shown that the increase of increase of silicon content in cast iron results in the increase of nucleation potential of graphite ($N_{V,cr}$), temperature range, (ΔT_{sc}) and the decrease of growth coefficient (μ) as well as the pre-eutectic austenite volume fraction (f_γ). Such variations lead to decrease of the absolute chilling tendency (CT) and in consequence to decrease of chills in cast iron. It has been also shown that intensity of silicon influence on the absolute chilling tendency and width of chill become smaller and smaller when its content in cast iron increases.

REFERENCES

[1] A. G. Fuller, Effect of superheating on chill and mottle formation. B.C.I.R.A Journal of Research and Development **9**, 693-708 (1961).

[2] J. W. Boyes, A. G. Fuller, Chill and Motlle formation in cast iron, B.C.I.R.A Journal of Research and Development **12**, 424-431 (1964).

[3] N. Girshovitz, Solidification and properties of cast iron (in russian). Mashinostroyene, Moscow-Leningrad (1966).

[4] J. V. Dawson, S. Maitra, Recent research on the inoculation of cast iron, British Foundrymen **4**, 117-127 (1976).

[5] H. D. Merchant, Solidification of Cast Iron. in: Recent Research on Cast Iron, Gordon and Breach, H. Merchant editors, Science Publishers, New York, 1-100 (1968).

[6] E. Fraś, T. Serano, A. Bustos, Fundiciones de Hierro, ILAFA, Chile (1990).

[7] E. J. Kubick, A. Javaid, F. J. Bradley, Investigation on Effect C, Si, Mn, S and P on Solidification Characteristics and Chill Tendency of Gray Iron – Part II: Chill Tendency, AFS Transaction **103**, 579-586 (1997).

[8] E. J. Kubick, A. Javaid, F. J. Bradley, Investigation of effect of C, Si, Mn, S and P on solidification characteristic and chill tendency of gray iron-Part I: Thermal Analysis Results, AFS, Transactions **105**, 573-578 (1997).

[9] W. Oldfield, The chill-reducing mechanism of silicon in cast iron. B.C.I.R.A Journal of Research and Development **10**, 17-27 (1962).

[10] M. Hillert, V. V. Subba Rao, Grey and white solidification of cast iron. in The Solidification of Metals. The Institute of Metals, London **110**, 204-212 (1968).

[11] P. Magnin, W. Kurz, Transition from grey to white and to grey in Fe-C-X eutectic alloys. In The Physical Metallurgy of Cast Iron, H. Fredrickson and M. Hillert editors, North Holland, New York, 263-272 (1985).

[12] H. Fredriksson, I. L. Svenson, Computer simulation of the structure formed during solidification of cast iron. in The Physical Metallurgy of Cast Iron, H. Fredrickson and M. Hillert editors, North Holland, New York, 273-284 (1985).

[13] L. Nastac, D. M. Stefanescu, Prediction of grey-to-white transition in cast iron by solidification modelling. AFS Transaction **103**, 329-337 (1995).

[14] L. Nastac, D. M. Stefanescu, Modelling of stable-to-metastable structural transition in cast iron, in Physical Metallurgy of Cast Iron V, G. Lesoult and J. Lacaze editors. Scitec Publications, Switzerland, 469-484 (1997).

[15] J. Rys, Stereology of materials, Fotobit, Cracov, 1995.

[16] J. Osher, U. Lorz, Quantitative Gefuengenanalysie, DVG Leipzig-Stuttgard, 1994.

[17] E. Fras, M. Górny, H. Lopez, The Transition from Gray to White Iron during Solidification **36A**, (2005).

[18] B. Lux, K. Kurz, Eutectic Growth of Iron-Carbon -Silicon and Iron-Carbon-Silicon-Sulphur Alloys, in Solidification of Metals. The Iron and Steel Institute, London, 193-198 (1967).

[19] P. Magnin, W. Kurz, Transition from grey to white and to grey in Fe-C-X eutectic alloys. In The Physical Metallurgy of Cast Iron, H. Fredrickson and M. Hillert editors, North Holland, New York, 263-272 (1985).

Received: 20 May 2008.